Harmonic Torque and Speed Pulsations in a Rectifier-Inverter Induction Motor Drive

THOMAS A. LIPO, MEMBER, IEEE, PAUL C. KRAUSE, SENIOR MEMBER, IEEE, AND HOWARD E. JORDAN, SENIOR MEMBER, IEEE

***Abstract*—A method of predicting the 6th-harmonic electromagnetic torque of an induction motor arising from a rectifier-inverter power source is presented. This study includes both the effects of harmonic variation rotor speed and inverter voltage. Although only the 6th harmonic is considered, it is shown that this is sufficiently accurate to predict steady-state system performance for practical speed ranges and system parameters. This investigation reveals that the 6th-harmonic electromagnetic torque pulsation may, at low frequencies, be significantly greater than that predicted by a constant speed, constant voltage analysis heretofore employed, and may materially affect the performance of the system.**

Paper 68 TP 638–PWR, recommended and approved by the Rotating Machinery Committee of the IEEE Power Group for presentation at the IEEE Summer Power Meeting, Chicago, Ill., June 23–28, 1968. Manuscript submitted February 12, 1968; made available for printing May 6, 1968. This work was made possible by a research grant from the Reliance Electric Company.

T. A. Lipo was with the Department of Electrical Engineering, University of Wisconsin, Madison, Wis. He is now with the Department of Electrical and Electronic Engineering, University of Manchester Institute of Science Technology, Manchester, England.

P. C. Krause is with the Department of Electrical Engineering, University of Wisconsin, Madison, Wis. 53706.

H. E. Jordan is with the Reliance Electric Company, Cleveland, Ohio.

Introduction

THE increasing use of variable frequency drive systems has resulted in many new application problems relating to the performance of an induction motor. One problem of importance in the application of a rectifier-inverter induction motor drive is that of the system instability which may occur at low frequencies. It has been shown that instability can occur over a wide speed range if the system parameters are improperly selected [1]. Other problems are related to the fact that most of the solid-state variable frequency power supplies provide a voltage source rich in harmonics. One obvious concern is the resulting increase in motor losses. This problem has been discussed in some detail by Klingshirn and Jordan [2].

Another concern which can prove equally troublesome is the pulsation of rotor speed due to the voltage harmonics applied to the machine when driven from an inverter supply. In applications where uniform speed of rotation is mandatory, such as machine tool, antenna positioning, and other applications, it is important to establish a method for obtaining the magnitude of these speed oscillations. This problem differs from that of system instability in that the torque pulsation and the resulting speed oscillation is a natural consequence of the inverter voltage waveshape rather than a result of an improper choice of system parameters. Although the system instability problem can be overcome by a choice of parameters, the steady-state torque pulsations cannot be eliminated. In many cases these torque pulsations define the lower limit of the speed range which yields satisfactory system performance.

In previous studies considerable attention has been given to calculating these electromagnetic torque harmonics. Jain [3], by neglecting stator resistance, has established a general equation for the average torque for an arbitrary balanced set of applied voltages. Ward *et al.* [4] have derived an instantaneous expression for the electromagnetic torque by calculating the four eigenvalues of the system characteristic equation. Sabbagh and Shewan [5] also developed an expression for the instantaneous electromagnetic torque by means of the instantaneous symmetrical component transformation. In this paper both the continuous and discontinuous stator current modes of operation were considered. Krause [6] by means of appropriate reference frames has reduced the calculations of instantaneous torque during the continuous current mode of operation to an algebraic process. In all of these studies the equations describing system operation have been linearized by assuming a constant rotor speed as well as a constant inverter (dc) voltage. The constant speed constraint was required in these calculations so that superposition could be employed.

In an actual system neither the rotor speed nor terminal voltage is constant. The harmonic torques acting on the rotor of the induction machine produce an oscillation in rotor speed, and the harmonic components of stator current result in a harmonic variation in inverter voltage. Although these effects can be neglected for higher frequency operation, they may become appreciable at low frequencies. In this paper an analytical method for calculating the induction motor pulsating torques arising from a rectifier-inverter power source is given. This analysis is general in that it includes both the effects of steady-state speed variations and voltage fluctuations. The results obtained employing this method of analysis are verified by a comparison with the results obtained from a hybrid computer simulation. It is shown that these speed and voltage variations have a significant effect on the magnitude of the steady-state electromagnetic torque pulsation at low frequencies.

System Representation

A circuit diagram of the system under consideration is given in Fig. 1. This idealized variable speed drive is identical to the system studied in a companion paper [7]. In brief, the system consists of a three-phase power source, a six-phase rectifier with associated filter, a three-phase inverter, and a three-phase symmetrical induction machine. The system is operated open loop without feedback control.

In the companion paper a general set of equations is derived for this type of drive system which includes voltage and current harmonics. For convenience these general equations are summarized in this section. The equations which describe the symmetrical induction machine in the synchronously rotating reference frame may be expressed [8] as follows:

$$\begin{bmatrix} v_{qs} \\ v_{ds} \\ 0 \\ 0 \end{bmatrix} = \begin{bmatrix} r_s + (p/\omega_b)X_s & f_R X_s & (p/\omega_b)X_m & f_R X_m \\ -f_R X_s & r_s + (p/\omega_b)X_s & -f_R X_m & (p/\omega_b)X_m \\ (p/\omega_b)X_m & f_R S X_m & r_r' + (p/\omega_b)X_r' & f_R S X_r' \\ -f_R S X_m & (p/\omega_b)X_m & -f_R S X_r' & r_r' + (p/\omega_b)X_r' \end{bmatrix} \times \begin{bmatrix} i_{qs} \\ i_{ds} \\ i_{qr}' \\ i_{dr}' \end{bmatrix} \quad (1)$$

where

$$S = (\omega_e - \omega_r)/\omega_e \quad (2)$$

$$f_R = \omega_e/\omega_b \quad (3)$$

and p denotes differentiation with respect to time. In this equation the superscript e has been omitted from the voltage and current variables since only the synchronously rotating reference frame is used in this analysis.

In (1), ω_e denotes the angular velocity of the synchronously rotating reference frame, ω_r denotes the equivalent electrical angular velocity of the rotor, ω_b represents the base or reference angular velocity used to establish a per unit system. Since f_R is defined as the ratio of the applied electrical frequency to the base frequency, it can be interpreted as the per unit operating frequency. Also, in (1) the angular relationship between the q axis and the magnetic axes of the stator and rotor phases has been selected so that these axes coincide at time zero. The electromagnetic torque expressed in per unit and positive for motor action is

$$T_e = X_m(i_{qs}i_{dr}' - i_{ds}i_{qr}'). \quad (4)$$

The dynamics of the mechanical system is described by

$$T_e - T_L = (2H/\omega_b)p\omega_r. \quad (5)$$

The stator voltage and current variables referred to the synchronously rotating reference frame may be expressed in terms of inverter variables as [7]

$$v_{qs} = V_I'(1 + \tfrac{2}{35}\cos 6\omega_e t - \tfrac{2}{143}\cos 12\omega_e t + \cdots) \quad (6)$$

$$v_{ds} = V_I'(\tfrac{12}{35}\sin 6\omega_e t - \tfrac{24}{143}\sin 12\omega_e t + \cdots) \quad (7)$$

$$I_I' = i_{qs}(1 + \tfrac{2}{35}\cos 6\omega_e t - \tfrac{2}{143}\cos 12\omega_e t + \cdots) + i_{ds}(\tfrac{12}{35}\sin 6\omega_e t - \tfrac{24}{143}\sin 12\omega_e t + \cdots). \quad (8)$$

The voltage equations for the rectifier and filter, valid during continuous operation ($I_R \neq 0$) may be written

$$V_{Ro}' = V_I' + [(p/\omega_b)X_{LF}' + R_{LF}' + X_{co}']I_R'. \quad (9)$$

$$V_I' = (\omega_b/p)X_{CF}'(I_R' - I_I'). \quad (10)$$

In (6)–(10) the filter quantities have been referred to the stator winding of the machine. This is accomplished by defining the primed variables as

$$V_I' = (2/\pi)V_I \quad (11)$$

$$V_{Ro}' = (2/\pi)V_{Ro} = (6\sqrt{3}/\pi^2)V_S\cos\alpha \quad (12)$$

$$I_I' = (\pi/3)I_I \quad (13)$$

$$I_R' = (\pi/3)I_R \quad (14)$$

$$X_{CF}' = (6/\pi^2)X_{CF} \quad (15)$$

$$X_{LF}' = (6/\pi^2)X_{LF} \quad (16)$$

$$R_{LF}' = (6/\pi^2)R_{LF} \quad (17)$$

$$X_{co}' = (18/\pi^3)X_{co}. \quad (18)$$

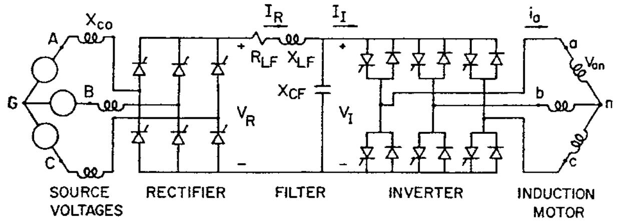

Fig. 1. System studied.

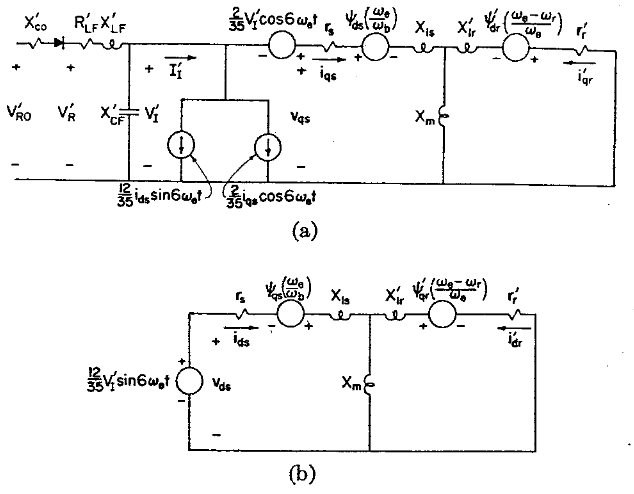

Fig. 2. Equivalent circuit of rectifier-inverter induction motor drive which includes effect of 5th and 7th stator-voltage harmonics. (a) q axis. (b) d axis.

Derivation of the 6th-Harmonic Torque

Equations (1) and (4)–(10) comprise a set which completely describe the behavior of a rectifier-inverter induction motor drive. However, due to the infinite series of time-varying coefficients in (6)–(8) it is desirable to simplify these equations to a set which closely approximates the actual system response.

At higher inverter frequencies the harmonic content of the applied stator voltages and the resulting harmonic currents are shown in the companion paper to have negligible effect on system performance [7]. At sufficiently low frequencies the harmonic coefficients in (6)–(8) begin to influence system response and cannot be neglected. However, unless the inverter frequency is nearly zero, the 5th and 7th harmonics predominate and the effect of the 11th, 13th, and higher stator voltage and current harmonics may be neglected.

In the synchronously rotating reference frame the 5th and 7th harmonics are transformed to 6th-harmonic quantities. If it is assumed that only the 6th-harmonic terms in (6)–(8) appreciably affect the behavior of the system, a rectifier-inverter drive may be conveniently represented by the equivalent circuit shown in Fig. 2. This equivalent circuit is similar to the one given in the companion paper. However, in Fig. 2 only the 5th and 7th harmonics of stator voltage have been incorporated into representation as dependent voltage and current generators. It is clear that an equivalent circuit can be constructed for any degree of accuracy by simply adding additional voltage and current generators.

If the static drive system is stable, the steady-state voltage and current quantities referred to the synchronously rotating reference frame, the rotor speed as well as the inverter voltage and current consist of a constant component plus 6th, 12th, and larger multiples of the 6th harmonic. Since the 12th and higher harmonics are neglected, all variables may be written as a sum of a constant plus a 6th-harmonic component. For example,

$$V_I' = V_{Io}' + V_{I6}' = V_{Io}' + V_{I\alpha}' \cos 6\omega_e t + V_{I\beta}' \sin 6\omega_e t \qquad (19)$$

$$I_I' = I_{Io}' + I_{I6}' = I_{Io}' + I_{I\alpha}' \cos 6\omega_e t + I_{I\beta}' \sin 6\omega_e t \qquad (20)$$

$$T_e = T_{eo} + T_{e6} = T_{eo} + T_{e\alpha} \cos 6\omega_e t + T_{e\beta} \sin 6\omega_e t \qquad (21)$$

$$\omega_r = \omega_{ro} + \omega_{r6} = \omega_{ro} + \omega_{r\alpha} \cos 6\omega_e t + \omega_{r\beta} \sin 6\omega_e t \qquad (22)$$

$$v_{qs} = v_{qso} + v_{qs6} = v_{qso} + v_{qs\alpha} \cos 6\omega_e t + v_{qs\beta} \sin 6\omega_e t \qquad (23)$$

$$i_{qs} = i_{qso} + i_{qs6} = i_{qso} + i_{qs\alpha} \cos 6\omega_e t + i_{qs\beta} \sin 6\omega_e t \qquad (24)$$

and so forth for v_{ds}, i_{ds}, i_{dr}', i_{qr}', and I_R'. Substituting these quantities into (1) and (4)–(10) yields a set of equations containing only a dc, 6th-harmonic and 12th-harmonic terms. Equating terms of the same frequency yields three sets of equations; one set containing dc terms only, one set containing 6th-harmonic terms, and one set involving only 12th-harmonic quantities. Since only the 6th-harmonic torque is of interest in this development, the set of equations containing the 12th-harmonic terms will not be considered.

The set of equations having only dc terms are

$$\begin{bmatrix} v_{qso} \\ v_{dso} \\ 0 \\ 0 \end{bmatrix} = \begin{bmatrix} r_s & f_R X_s & 0 & f_R X_m \\ -f_R X_s & r_s & -f_R X_m & 0 \\ 0 & f_R S_o X_m & r_r' & f_R S_o X_r' \\ -f_R S_o X_m & 0 & -f_R S_o X_m & r_r' \end{bmatrix} \times \begin{bmatrix} i_{qso} \\ i_{dso} \\ i_{qro}' \\ i_{dro}' \end{bmatrix}$$

$$+ \left(\frac{1}{2\omega_b}\right) \begin{bmatrix} 0 & 0 & 0 & 0 & 0 & 0 & 0 & 0 \\ 0 & 0 & 0 & 0 & 0 & 0 & 0 & 0 \\ 0 & 0 & \omega_{r\alpha} X_m & \omega_{r\beta} X_m & 0 & 0 & \omega_{r\alpha} X_r' & \omega_{r\beta} X_r' \\ -\omega_{r\alpha} X_m & -\omega_{r\beta} X_m & 0 & 0 & -\omega_{r\alpha} X_r' & -\omega_{r\beta} X_r' & 0 & 0 \end{bmatrix} \times \begin{bmatrix} i_{qs\alpha} \\ i_{qs\beta} \\ i_{ds\alpha} \\ i_{ds\beta} \\ i_{qr\alpha}' \\ i_{qr\beta}' \\ i_{dr\alpha}' \\ i_{dr\beta}' \end{bmatrix} \qquad (25)$$

where

$$S_o = (\omega_e - \omega_{ro})/\omega_e \tag{26}$$

$$T_{eo} = X_m[i_{qso}i_{dro}' - i_{dso}i_{qro}' + \tfrac{1}{2}(i_{qs\alpha}i_{dr\alpha}' + i_{qs\beta}i_{dr\beta}' - i_{ds\alpha}i_{qr\alpha}' - i_{ds\beta}i_{qr\beta}')] \tag{27}$$

$$T_{eo} - T_{Lo} = 0 \tag{28}$$

$$v_{qso} = V_{Io}' + \tfrac{1}{35}V_{I\alpha}' \tag{29}$$

$$v_{dso} = \tfrac{6}{35}V_{I\beta}' \tag{30}$$

$$I_{Io}' = i_{qso} + \tfrac{1}{35}i_{qs\alpha} + \tfrac{6}{35}i_{ds\beta} \tag{31}$$

$$V_{Ro}' = V_{Io}' + (R_{LF}' + X_{co}')I_{Ro}' \tag{32}$$

$$0 = I_{Ro}' - I_{Io}'. \tag{33}$$

The zero quantities and the magnitude of the 6th-harmonic quantities together make up the steady-state operating point. However, for normal operation the zero quantities are much larger than the magnitude of the 6th-harmonic quantities which do not contribute appreciably to the average values of the system variables. This fact has been noted by other investigators [9].

$$\begin{bmatrix} v_{qs6} \\ v_{ds6} \\ 0 \\ 0 \end{bmatrix} = \begin{bmatrix} r_s + (p/\omega_b)X_s & f_R X_s & (p/\omega_b)X_m & f_R X_m & 0 \\ -f_R X_s & r_s + (p/\omega_b)X_s & -f_R X_m & (p/\omega_b)X_m & 0 \\ (p/\omega_b)X_m & f_R S_o X_m & r_r' + (p/\omega_b)X_r' & f_R S_o X_m & X_m i_{dso} + X_r' i_{dro}' \\ -f_R S_o X_m & (p/\omega_b)X_m & -f_R S_o X_r' & r_r' + (p/\omega_b)X_r' & -(X_m i_{qso} + X_r' i_{qro}') \end{bmatrix} \times \begin{bmatrix} i_{qs6} \\ i_{ds6} \\ i_{qr6}' \\ i_{dr6}' \\ \omega_{r6}/\omega_b \end{bmatrix} \tag{41}$$

Hence (25), (27), and (29)–(31) may be expressed approximately as

$$\begin{bmatrix} v_{qso} \\ v_{dso} \\ 0 \\ 0 \end{bmatrix} = \begin{bmatrix} r_s & f_R X_s & 0 & f_R X_m \\ -f_R X_s & r_s & -f_R X_m & 0 \\ 0 & f_R S_o X_m & r_r' & f_R S_o X_r' \\ -f_R S_o X_m & 0 & -f_R S_o X_r' & r_r' \end{bmatrix} \times \begin{bmatrix} i_{qso} \\ i_{dso} \\ i_{qro}' \\ i_{dro}' \end{bmatrix} \tag{34}$$

$$T_{eo} = X_m(i_{qso}i_{dro}' - i_{dso}i_{qro}') \tag{35}$$

$$v_{qso} = V_{Io}' \tag{36}$$

$$v_{dso} = 0 \tag{37}$$

$$I_{Io}' = i_{qso}. \tag{38}$$

Upon simplifying, the steady-state constant quantities (dc terms) can be expressed simply as

$$\begin{bmatrix} V_{Ro}' \\ 0 \\ 0 \\ 0 \end{bmatrix} = \begin{bmatrix} r_s + R_{LF}' + X_{co}' & f_R X_s & 0 & f_R X_m \\ -f_R X_s & r_s & -f_R X_m & 0 \\ 0 & f_R S_o X_m & r_r' & f_R S_o X_r' \\ -f_R S_o X_m & 0 & -f_R S_o X_r' & r_r' \end{bmatrix} \times \begin{bmatrix} i_{qso} \\ i_{dso} \\ i_{qro}' \\ i_{dro}' \end{bmatrix} \tag{39}$$

$$T_{Lo} = X_m(i_{qso}i_{dro}' - i_{dso}i_{qro}'). \tag{40}$$

It is clear that (39) and (40) formulate an algebraic set of equations which establish the average value of all variables. Although these equations are approximate, it will be shown that they are sufficiently accurate to approximate the average value of the converter and machine variables.

Equating terms for the 6th harmonic yields

$$T_{e6} = X_m(i_{qso}i_{dr6}' + i_{dro}'i_{qs6} - i_{qro}'i_{ds6} - i_{dso}i_{qr6}') \tag{42}$$

$$\frac{\omega_{r6}}{\omega_b} = \frac{1}{2Hp}T_{e6} \tag{43}$$

$$v_{qs6} = \tfrac{2}{35}V_{Io}' \cos 6\omega_e t + V_{I6}' \tag{44}$$

$$v_{ds6} = \tfrac{12}{35}V_{Io}' \sin 6\omega_e t \tag{45}$$

$$I_{I6}' = i_{qs6} + \tfrac{2}{35}i_{qso}\cos 6\omega_e t + \tfrac{12}{35}i_{dso}\sin 6\omega_e t \tag{46}$$

$$0 = V_{I6}' + \left(\frac{p}{\omega_b}X_{LF}' + R_{LF}' + X_{co}'\right)I_{I6}' \tag{47}$$

$$V_{I6}' = \frac{\omega_b}{p}X_{CF}'(I_{R6}' - I_{I6}'). \tag{48}$$

Equations (41)–(48) form a linear set of eleven equations having eleven unknown quantities. In these equations the zero subscripted quantities can be treated as known constants since they may be determined by (39)–(40). Moreover, the four forcing functions, namely,

$$\tfrac{2}{35}V_{Io}'\cos 6\omega_e t,\quad \tfrac{12}{35}V_{Io}'\sin 6\omega_e t,\quad \tfrac{2}{35}i_{qso}\cos 6\omega_e t,\quad \tfrac{12}{35}i_{dso}\sin 6\omega_e t$$

are of the same frequency. Hence all variables in the steady state will be of this frequency and phasors may be employed. Therefore, if $\cos 6\omega_e t$ is replaced by 1, $\sin 6\omega_e t$ by $-j$, p/ω_b by $j6f_R$, and after some simplification, (41) and (48) become

$$\begin{bmatrix} V_{I6} + \frac{2}{35}V_{Io}' \\ -j\frac{12}{35}V_{Io}' \\ 0 \\ 0 \end{bmatrix} = \begin{bmatrix} r_s + j6f_RX_s & f_RX_s & j6f_RX_m & f_RX_m & 0 \\ -f_RX_s & r_s + j6f_RX_s & -f_RX_m & j6f_RX_m & 0 \\ j6f_RX_m & f_RS_oX_m & r_r' + j6f_RX_r' & f_RS_oX_r & X_mi_{dso} + X_r'i_{dro}' \\ -f_RS_oX_m & j6f_RX_m & -f_RS_oX_r' & r_r' + j6f_RX_r' & -(X_mi_{qso} + X_r'i_{qro}') \end{bmatrix} \times \begin{bmatrix} \bar{\imath}_{qs6} \\ \bar{\imath}_{ds6} \\ \bar{\imath}_{qr6}' \\ \bar{\imath}_{dr6}' \\ \bar{\omega}_{r6}/\omega_b \end{bmatrix} \quad (49)$$

$$\frac{\bar{\omega}_{r6}}{\omega_b} = \frac{-jX_m}{12Hf_R\omega_b}(i_{qso}\bar{\imath}_{dr6}' + i_{dro}'\bar{\imath}_{qs6} - i_{qro}'\bar{\imath}_{ds6} - i_{dso}\bar{\imath}_{qr6}') \quad (50)$$

$$\bar{I}_{I6}' = \bar{\imath}_{qs6} + \tfrac{2}{35}i_{qso} - j\tfrac{12}{35}i_{dso} \quad (51)$$

$$\bar{V}_{I6}' = -j\frac{X_{CF}'}{6f_R}(\bar{I}_{R6}' - \bar{I}_{I6}'). \quad (52)$$

The bar over the variables is used to denote complex or phasor quantities. Eliminating $\bar{I}_{R6}'$ from (51) and (52) yields

$$\bar{V}_{I6}' = \frac{-X_{CF}'(R_{LF}' + j6f_RX_{LF}')}{(X_{CF}' - 36f_R^2X_{LF}') + j6f_RR_{LF}'}\bar{I}_{I6}' \quad (53)$$

or simply

$$\bar{V}_{I6}' = -(R_{F6} + jX_{F6})\bar{I}_{I6}'. \quad (54)$$

The 6th-harmonic inverter current $\bar{I}_{I6}'$ in (51) may be eliminated by means of (54). Thus

$$\bar{V}_{I6} = -(R_{F6} + jX_{F6})\bar{\imath}_{qs6} - \tfrac{2}{35}(R_{F6}i_{qso} + 6X_{F6}i_{dso}) + j\tfrac{2}{35}(6R_{F6}i_{dso} - X_{F6}i_{qso}). \quad (55)$$

Substituting (32), (50), and (55) into the matrix (49) yields the final result

$$\begin{bmatrix} \frac{2}{35}[V_{Ro}' - (R_{F6} + R_{LF}' + X_{co}')i_{qso} - 6X_{F6}i_{dso} + j(6R_{F6}i_{dso} - X_{F6}i_{qso})] \\ -j\frac{12}{35}[V_{Ro}' - (R_{LF}' + X_{co}')i_{qso}] \\ 0 \\ 0 \end{bmatrix}$$

$$= \begin{bmatrix} r_s + R_{F6} + j(6f_RX_s + X_{F6}) & f_RX_s & j6f_RX_m & f_RX_m \\ -f_RX_s & r_s + jf_RX_s & -f_RX_m & j6f_RX_m \\ j(K_T\psi_{dro}i_{dro}' + 6f_RX_m) & f_RS_oX_m - jK_T\psi_{dro}i_{qro}' & r_r' + j(6f_RX_r' - K_T\psi_{dro}i_{dso}) & f_RS_oX_r' + jK_T\psi_{dro}i_{qso} \\ -f_RS_oX_m - jK_T\psi_{qro}i_{dro}' & j(6f_RX_m + K_T\psi_{qro}i_{qro}') & -f_RS_oX_r' + jK_T\psi_{qro}i_{dso} & r_r' + j(6f_RX_r' - K_T\psi_{qro}i_{qso}) \end{bmatrix} \times \begin{bmatrix} \bar{\imath}_{qs6} \\ \bar{\imath}_{ds6} \\ \bar{\imath}_{qr6}' \\ \bar{\imath}_{dr6}' \end{bmatrix}. \quad (56)$$

where the following substitute quantities are used for convenience

$$\psi_{qro} = X_mi_{qso} + X_r'i_{qro}' \quad (57)$$

$$\psi_{dro} = X_mi_{dso} + X_r'i_{dro}' \quad (58)$$

$$K_T = X_m/12f_R\omega_bH. \quad (59)$$

Equation (56) may be written in abbreviated form as

$$\bar{\boldsymbol{v}}_6 = \bar{\boldsymbol{Z}}\bar{\boldsymbol{\imath}}_6 = (\boldsymbol{R} + j\boldsymbol{X})\bar{\boldsymbol{\imath}}_6. \quad (60)$$

It is clear that $\boldsymbol{R}$ and $\boldsymbol{X}$ denote the real and imaginary parts of the complex impedance matrix $\bar{\boldsymbol{Z}}$ defined in (56), $\bar{\boldsymbol{v}}_6$ and $\bar{\boldsymbol{\imath}}_6$ the voltage and current column vectors in (56). Inverting this matrix yields [1]

$$\bar{\boldsymbol{\imath}}_6 = (\boldsymbol{G} + j\boldsymbol{B})\bar{\boldsymbol{v}}_6 \quad (61)$$

where

$$\boldsymbol{G} = \boldsymbol{X}^{-1}\boldsymbol{R}(\boldsymbol{X} + \boldsymbol{R}\boldsymbol{X}^{-1}\boldsymbol{R})^{-1} \quad (62)$$

$$\boldsymbol{B} = -(\boldsymbol{X} + \boldsymbol{R}\boldsymbol{X}^{-1}\boldsymbol{R})^{-1}. \quad (63)$$

In complex form the 6th-harmonic per unit torque $\bar{T}_{e6}$ is given by

$$\bar{T}_{e6} = X_m[i_{dro}', -i_{qro}', -i_{dso}, i_{qso}]\cdot\bar{\boldsymbol{\imath}}_6 \quad (64)$$

where the dot denotes the inner product of the row and column vector. The magnitude of the 6th-harmonic torque is expressed as follows:

$$|\bar{T}_{e6}| = [\mathrm{Re}\,(\bar{T}_{e6})^2 + \mathrm{Im}\,(\bar{T}_{e6})^2]^{1/2}. \quad (65)$$

Thus from (43) the magnitude of the per unit 6th-harmonic speed deviation is

$$\left|\frac{\bar{\omega}_{r6}}{\omega_b}\right| = \frac{1}{12f_R\omega_b}|\bar{T}_{e6}|. \quad (66)$$

In some applications it may be more direct to express the 6th-harmonic speed deviation as a fraction of the applied electrical frequency rather than of a base frequency. In this case

$$\left|\frac{\bar{\omega}_{r6}}{\omega_e}\right| = \frac{1}{12f_R^2\omega_b}|\bar{T}_{e6}|. \quad (67)$$

Equation (56) formulates a linear matrix equation which includes the effect of the speed deviation and the fluctuation of terminal voltage in the calculation of the 6th-harmonic torque pulsation. The effect of speed deviation is taken into account

TABLE I

Figures	r_s	r_r'	X_s	X_r'
3–10	0.025	0.020	2.075	2.075
Figures	X_m	X_{LF}	R_{LF}	X_{co}
3–10	2.0	0.5	0.025	0.016
Figures	X_{CF}	H	V_{Ro}'	
3	...	...	$1.2f_R$	
4	...	0.2	$1.2f_R$	
5	0.00705	0.2	$1.2f_R$	
6	varied	0.2	0.12	
7	0.0141	0.2	0.12	
8	0.0141	0.2	0.12	
9	0.0564	0.2	0.12	
10	0.0564	0.2	0.12	

by appropriate terms in the impedance coefficients of the third and fourth row of (56). The effect of voltage fluctuation is included by quantities in the elements of the voltage vector and the (1, 1) element of the impedance matrix.

Comparison of Results

The equations which have been developed offer a means of predicting the magnitude of the 6th-harmonic torque pulsation arising in one type of rectifier-inverter induction motor drive. Although these equations are valid for any frequency, they are especially significant at low operating frequencies, where the rotor speed and terminal voltage can no longer be assumed constant. In the following results 60 Hz is assumed to be the base frequency, and the per unit system is based upon operation at this frequency ($\omega_b = 377$ rad/s).

In variable speed systems, the amplitude of the applied stator voltages is decreased as the frequency decreases. If the terminal voltage of the machine is decreased so as to maintain a constant volts per hertz the breakdown torque of the machine is depleted considerably at low frequency. In some applications it may be desirable to adjust the terminal voltage so as to maintain a constant breakdown torque. In this case a regulator would be required to maintain a constant flux level in the machine. This added boost is given the terminal voltage since the voltage drop across the stator resistance becomes a larger percent of the applied stator voltage as the frequency decreases. However, in this study it has been assumed that the system is operated open loop, and that the amplitude of the fundamental component of the open-circuit inverter voltage is decreased linearly with frequency. That is

$$v_{qso} = V_I' = f_R V_m \tag{68}$$

where, as an approximate means of low-frequency compensation, $V_m = 1.2$-pu voltage. This is accomplished by adjusting the normalized rectifier voltage V_{Ro}' so that

$$V_{Ro}' = 1.2 f_R. \tag{69}$$

In order to verify the approximate equations derived in the previous section, the equations which describe the dynamic performance of the rectifier, filter, inverter, and induction motor were simulated on a hybrid computer, and the results obtained from this simulation were compared to the results obtained using the approximate equation. The simulation of this system is discussed and verified in earlier papers wherein the rectifier is represented as a constant voltage V_{Ro}' in series with a normalized

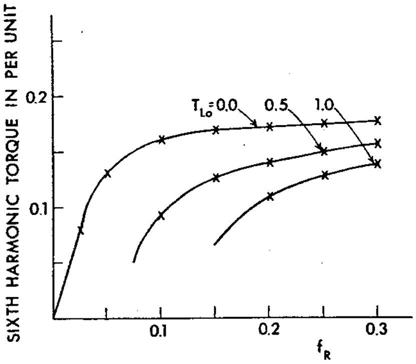

Fig. 3. Magnitude of 6th-harmonic torque for constant rotor speed and constant inverter voltage.

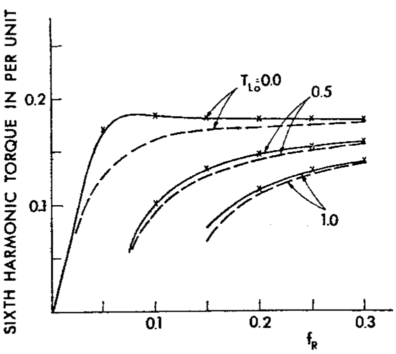

Fig. 4. 6th-harmonic torque magnitude including effects of change in speed.

commutating reactance X_{co}' and the inverter is simulated as an ideal switching device having negligible commutation period. The induction motor was represented in the stationary reference frame. The parameters of the system studied is given in Table I and are identical to those chosen in previous studies [1], [7], [10], [11]. These parameters are based on a 7.5-hp induction motor having a base impedance of 9.45 ohms. The value of filter capacitance $X_{CF} = 0.00705$ pu (40 000 μF) is sufficient to stabilize the machine over all regions of operation.

During the steady-state operation of the simulated system an on-line sampling was taken of the instantaneous electromagnetic torque obtained by the analog computer with an analog-to-digital converter. The sampling rate was sufficiently high to ensure three-decimal-point accuracy. Using the sampled value of the torque variable, a Fourier series was taken and the coefficient of the 6th harmonic extracted [13].

In order to clearly show the source of the harmonic torque pulsation, the system was first studied assuming that both the rotor speed ω_r and the inverter voltage V_I' were constant. This is readily accomplished by setting K_T, R_{F6}, and X_{F6} equal to zero in (56). A plot of the 6th-harmonic torque versus per unit frequency for three loading conditions obtained from a digital computer solution of the approximate equations is given in Fig. 3. The results from the hybrid computer solution using the Fourier series analysis is designated by an X in Fig. 3. Except for values of inertia and filter capacitance, all system parameters correspond to those given in Table I. The results obtained by a digital computer solution of (56) and (64) and the results obtained by the hybrid computer solution generally agree to three decimal places. In the digital computer solution the contri-

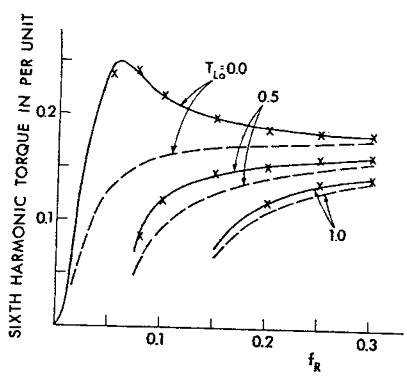

Fig. 5. Magnitude of 6th-harmonic torque including effects of change in speed and inverter voltage.

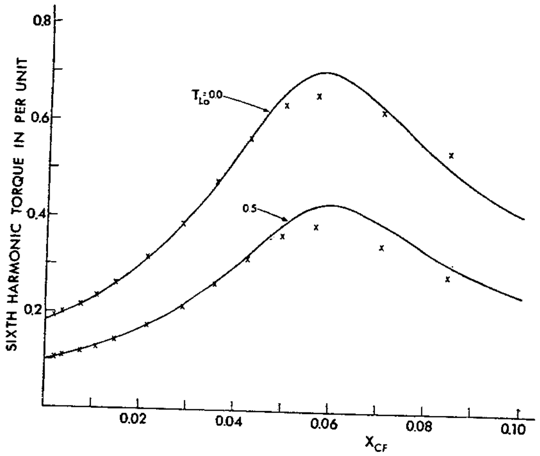

Fig. 6. 6th-harmonic torque magnitude for changes in filter capacitive reactance $f_R = 0.1$.

bution of the 5th, 7th, and higher harmonic components of stator and rotor currents have not been included in the calculation of average torque. Hence the close agreement obtained further justifies this approximation. As the per unit electrical frequency approaches zero the 6th-harmonic torque decreases indicating that the harmonic torques as well as the average value of torque tends toward zero for constant volts per hertz operation. The curves for $T_L = 0.5$ and 1.0 terminate at the frequency for which the breakdown torque is equal to this loading condition.

In Fig. 4 the constant speed constraint was removed and the inertia constant H set equal to 0.2 second as in Table I in both the digital and hybrid representation. The curves of Fig. 3 which shows the 6th-harmonic torque for operation at constant speed with a constant inverter voltage is included as dashed lines for comparison. The X denotes the results of the hybrid computer solution. Since the magnitude of the 6th-harmonic component of rotor speed is related directly to the 6th-harmonic torque pulsation, it is clear that the steady-state speed deviation could have been plotted rather than the 6th-harmonic torque by means of (66) or (67). It is noted from Fig. 4 that a 6th-harmonic oscillation in rotor speed results in an increase in the 6th-harmonic torque pulsation at low frequencies. The digital and hybrid results again generally agree to three decimal places over the frequency range considered.

In Fig. 5 the constant inverter voltage constraint was removed by setting the filter capacitive reactance $X_{CF} = 0.00705$ pu. Again the curves of Fig. 3 are shown as dashed lines for purposes of comparison. The solid line indicates the results obtained from the digital computer solution while the X's denote the results obtained from the hybrid computer simulation. The 6th-harmonic fluctuation in the inverter voltage produces an additional increase in the magnitude of the 6th-harmonic torque. It is noted that at $f_R = 0.05$ (3 Hz) and zero load torque, the pulsating component of torque is nearly twice that predicted by a constant voltage, constant speed analysis.

In Fig. 6 the per unit frequency f_R was set equal to 0.1 and the effect of a change of filter capacitance studied. The abscissa is scaled as a function of X_{CF}. Thus $X_{CF} = 0$ corresponds to the case of constant inverter voltage studied in Fig. 4 and $X_{CF} = 0.00705$ corresponds to the value of filter capacitance considered in Fig. 5. The results obtained from the digital computer solution are plotted as a solid line. An X denotes a point obtained by the hybrid computer solution. The torque pulsations increase to the point where the magnitude of the 6th-harmonic component of torque is over four times greater than a constant voltage, constant speed analysis would indicate. For capacitive reactances larger than this value, the harmonic torque pulsation decreases. However, in this region the 12th-harmonic component becomes appreciable, and the overall system performance is unacceptable.

Computer traces of system variables obtained from the hybrid computer solutions are given in Figs. 7–10. The unprimed filter variables are given rather than the primed variables defined in (11)–(18). In Fig. 7 the system is operating in the steady state with $f_R = 0.1$, $T_{Lo} = 0.0$, and $X_{CF} = 0.0141$ pu (20 000 μF). For this operating condition the average value of the 6th-harmonic component of inverter voltage is equal to about 10 percent of the average value. This is a severe oscillation for most practical systems. However, the correlation between the approximate digital computer method and the exact analog computer result agrees to nearly 1 percent.

Upon examination of the electromagnetic torque variable T_e, it is noted that this oscillation is almost entirely described by a 6th harmonic. In fact, computation of the 12th-harmonic component was, in most practical cases, beyond the accuracy range of the hybrid computer solution. The load torque has been changed to $T_{Lo} = 0.5$ in Fig. 8. Again, the results agree to within 1 percent.

In Fig. 9 the filter capacitive reactance has been changed to 0.0564 pu (5000 μF) while the loading condition and inverter frequency remain the same as Fig. 7. For this value of capacitance the 6th-harmonic torque pulsation is a maximum in Fig. 6. At this point fluctuation in inverter voltage is over 30 percent of the average value. Because of this large oscillation in inverter voltage the two methods only agree to within 7 percent. This is an extreme operating condition, however, and a practical system would not be designed with such a large deviation in terminal voltage. In addition, large values of capacitive reactance in the filter circuit generally result in a large region of unstable operation [1]. The computer traces shown in Fig. 10 illustrate a loading of 0.5 pu for the same system considered in Fig. 9. Again, the stator voltage and current are extremely distorted by the fluctuation in inverter voltage. The two methods of analysis differ in this case by 10 percent.

Conclusion

A method of determining the steady-state 6th-harmonic electromagnetic torque pulsation acting on the rotor of an induction machine when supplied from a rectifier-inverter source has been set forth. The effects of both changes of speed and changes in

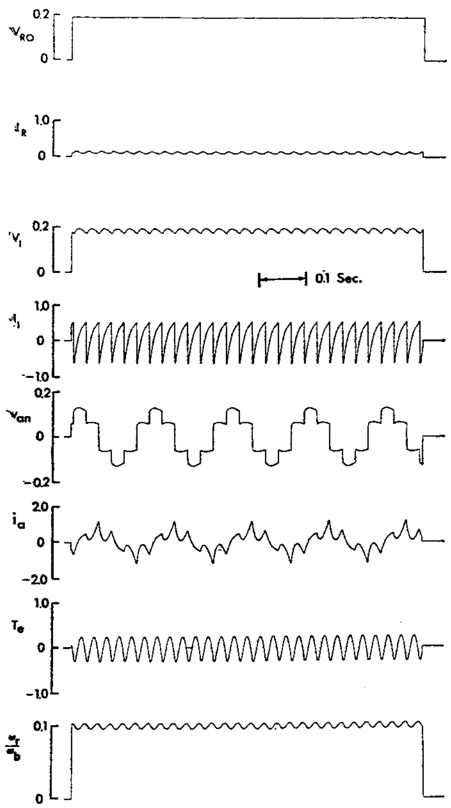

Fig. 7. Steady-state system variables for $X_{CF} = 0.0141$, $T_{Lo} = 0.0$. Results from hybrid computer study.

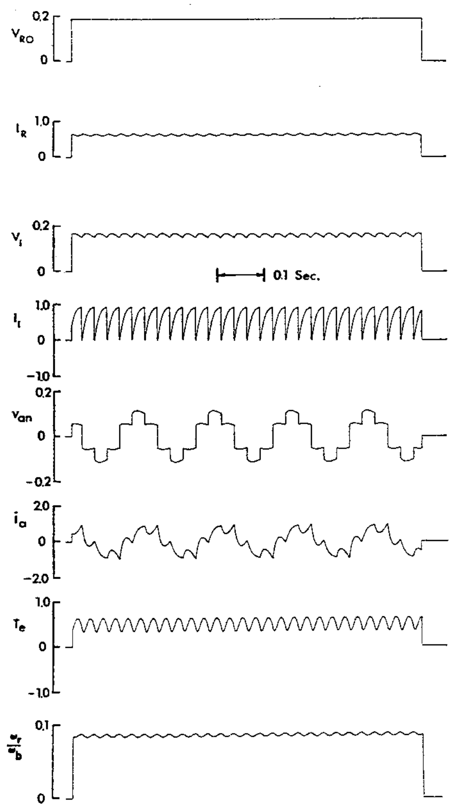

Fig. 8. Steady-state system performance for $X_{CF} = 0.0141$, $T_{Lo} = 0.5$. Results from hybrid computer study.

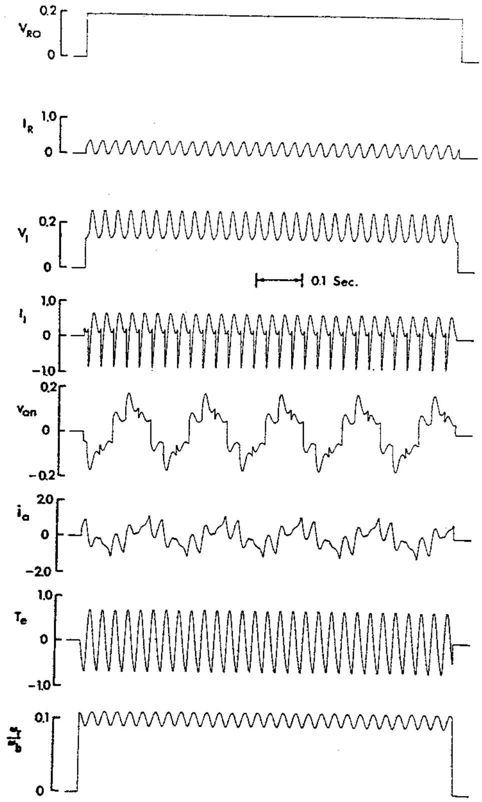

Fig. 9. Steady-state system performance for $X_{CF} = 0.0564$, $T_{Lo} = 0.0$. Results from hybrid computer solution.

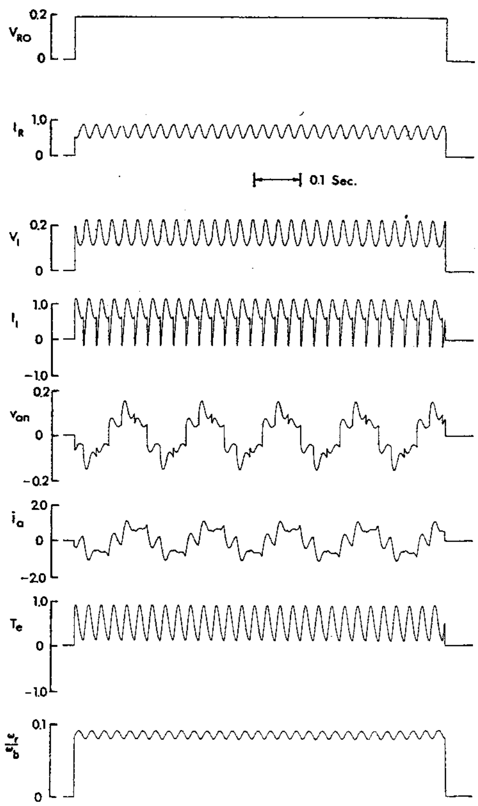

Fig. 10. Steady-state system variables for $X_{CF} = 0.0564$, $T_{Lo} = 0.5$. Results from hybrid computer solution.

inverter voltage have been incorporated in this analysis. However, the influence of the 12th and higher harmonics are not considered. It has been shown by means of a hybrid computer solution that these higher harmonics do not contribute appreciably to a speed oscillation.

In this paper only the influence of a change in the parameter X_{CF} was investigated in detail. It is clear that other parameters also significantly influence the magnitude of the 6th-harmonic torque pulsation. For example, the connected load provides damping and additional inertia to the system and tends to reduce the speed deviation, thus decreasing the torque pulsation. If the average value of rectifier voltage V_{Ro} is increased, the forcing function $\bar{\mathbf{v}}_6$ in (56) is increased, thus increasing the 6th-harmonic torque pulsation. Hence when the system is operated so as to maintain a constant breakdown torque, the harmonic torque components increase as well as the average torque component. In this case the magnitude of the 6th-harmonic component becomes increasingly large as zero frequency is approached.

It appears that the method of analysis presented herein is sufficient to predict the magnitude of the 6th-harmonic torque pulsation and subsequent speed oscillation to within 1 or 2 percent for practical system parameters and over typical speed ranges. It is shown that the 6th-harmonic fluctuation in inverter voltage and rotor speed have a significant effect on the magnitude of the steady-state 6th-harmonic torque. For practical systems this pulsation can at low frequencies typically become two or three times greater than that predicted by a classical constant speed, constant voltage analysis.

Acknowledgment

The computer studies were performed at the University of Wisconsin Hybrid Computer Laboratory, using equipment provided in part by an NSF grant.

References

[1] T. A. Lipo and P. C. Krause, "Stability analysis of a rectifier-inverter induction motor drive," *IEEE Trans. Power Apparatus and Systems*, vol. PAS-88, pp. 55–66, January 1969.
[2] E. A. Klingshirn and H. E. Jordan, "Polyphase induction motor performance and losses on nonsinusoidal voltage sources," *IEEE Trans. Power Apparatus and Systems*, vol. PAS-87, pp. 624–631, March 1968.
[3] G. C. Jain, "The effect of voltage waveshape on the performance of a 3-phase induction motor," *IEEE Trans. Power Apparatus and Systems*, vol. 83, pp. 561–566, June 1964.
[4] E. E. Ward, A. Kazi, and R. Farkas, "Time domain analysis of inverter-fed induction motor," *IEE Proc.* (London), vol. 114, pp. 361–369, March 1967.
[5] E. M. Sabbagh and W. Shewan, "Characteristics of an adjustable speed polyphase induction machine," *IEEE Trans. Power Apparatus and Systems*, vol. PAS-87, pp. 613–624, March 1968.
[6] P. C. Krause, "Method of multiple reference frames applied to the analysis of symmetrical induction machinery," *IEEE Trans. Power Apparatus and Systems*, vol. PAS-87, pp. 218–227, January 1968.
[7] P. C. Krause and T. A. Lipo, "Analysis and simplified representations of a rectifier-inverter induction motor drive," this issue, pp. 588–596.
[8] P. C. Krause and C. H. Thomas, "Simulation of symmetrical induction machinery," *IEEE Trans. Power Apparatus and Systems*, vol. PAS-84, pp. 1038–1053, November 1965.
[9] D. M. Mitchell and C. J. Triska, "An investigation of an SCR inverter drive for an induction motor," *Conference Record 1967 IEEE IGA Group Annual Meeting* (Pittsburgh, Pa.), pp. 81–90.
[10] P. C. Krause and L. T. Woloszyk, "Comparison of computer and test results of a static ac drive system," *IEEE Trans. Industry and General Applications*, vol. IGA-4, pp. 583–588, November/December 1968.
[11] L. T. Woloszyk, "An analog computer study of a static ac drive system," M. S. thesis, University of Wisconsin, Madison, 1967.
[12] R. A. Hedin, "The dynamic behavior of a synchronous generator with rectifier load," M. S. thesis, University of Wisconsin, Madison, 1964.
[13] D. E. Dick and H. J. Wertz, "Analog and digital computation of Fourier series and integrals," *IEEE Trans. Electronic Computers*, vol. EC-16, pp. 8-13, February 1967.